Organic LETTERS

Letter

pubs.acs.org/OrgLett

2,11-Dibromo-13,14-dimesityl-5,8-dioxapentaphene: A Stable and Twisted Polycyclic System Containing the *o*-Quinodimethane Skeleton

Chihiro Sato, Shuichi Suzuki, Masatoshi Kozaki,* and Keiji Okada*

Graduate School of Science, Osaka City University, 3-3-138 Sugimoto, Sumiyoshi-ku, Osaka 558-8585, Japan

Supporting Information

ABSTRACT: A stable *o*-quinodimethane (*o*QDM) derivative, 2,11-dibromo-13,14-dimesityl-5,8-dioxapentaphene (**3**) was synthesized, and its structure and properties were investigated. The X-ray structural analysis showed a significantly twisted π-framework and a clear bond-length alternation in the central *o*QDM skeleton. Owing to the quinoidal conjugation, **3** exhibited a broad absorption band in the visible region (up to 700 nm) and amphoteric redox behavior. Furthermore, radical cation $\mathbf{3}^{\bullet+}$ was isolated, and its electronic structure was elucidated by spectroscopic measurements.

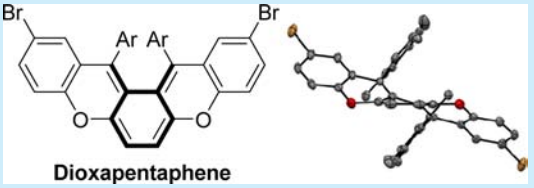

Synthesis of new π-conjugated frameworks with unique electrochemical and photophysical properties is important for the development of novel functional organic materials.[1] Quinodial π-conjugated systems are attractive building blocks because of their superior redox ability and wide absorption bands in the visible region.[2] In fact, *p*-quinodimethane (*p*QDM) derivatives have been extensively studied as electronic[3] and optical materials.[4] On the other hand, *o*-quinodimethane (*o*QDM) derivatives are well-known versatile reagents in synthetic chemistry due to their high reactivity.[5] *o*QDM derivatives are also promising functional organic materials,[6] even though the synthesis of stable derivatives is still challenging. Quinkert et al. reported that 7,7,8,8-tetraphenyl-*o*-quinodimethane (Ph_4*o*QDM) spontaneously isomerized into 1,1,2,2-tetraphenylbenzocyclobutene (**I**) and 4a,10-dihydro-9,10,10-triphenylanthracene (**II**) by intramolecular cyclization (Figure 1).[7] Suzuki et al. synthesized *o*QDM derivative **1** in which the cyclization of *o*QDM was suppressed by dibenzoannulation.[8] A phenanthrene-type framework was designed to destabilize the corresponding cyclized products by the steric congestion between the aryl units on the exocyclic carbons and hydrogen atoms at the 1,8-positions of phenanthrene. In the meantime, the dibenzoannulation generates a large local aromaticity in the outer benzene rings to reduce its quinoidal characteristics.[9,15a] Recently, Tobe et al. reported an air-stable *o*QDM derivative, indenofluorene **2**.[10] The two peripheral benzene rings in **2** were directly connected to the *o*QDM unit to inhibit the isomerization, and this extended *o*QDM skeleton showed a biradical nature.

We have designed 5,8-dioxapentaphene (DOP) as a new electron-rich π-conjugated system containing the *o*QDM structure. Two peripheral benzene rings in DOP were anchored to the central *o*QDM moiety with oxygen bridges that suppress the cyclization to the *o*QDM moiety. Moreover, DOP can be considered as two xanthyl units condensed together. Because xanthylium cation is a stable species, DOP is expected to form a stable cationic species.[11] Herein, we report the synthesis, structure, and properties of 2,11-dibromo-13,14-dimesityl-5,8-dioxapentaphene (**3**). Furthermore, we successfully isolated radical cation salt $\mathbf{3}^{\bullet+}\cdot SbF_6^-$. To the best of our knowledge, this is the first report on the structure and electronic properties of an *o*QDM-based radical cation.

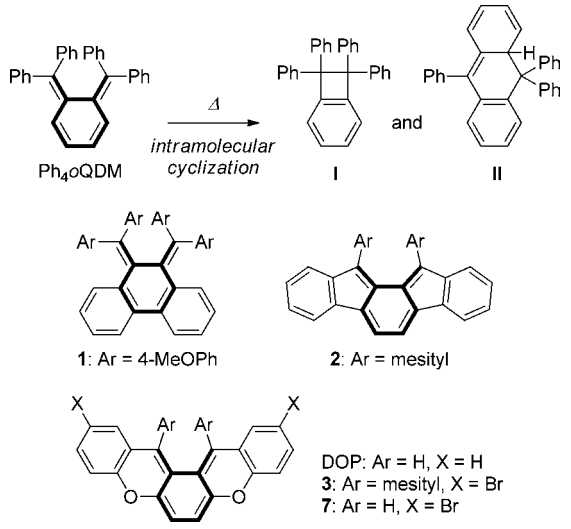

Figure 1. Chemical structures of Ph_4*o*QDM, **I**, **II**, **1**–**3**, and **7**.

Compound **3** was synthesized in five steps from 1,4-hydroquinone, as shown in Scheme 1. First, the nucleophilic substitution of 5-bromo-2-fluorobenzonitrile with 1,4-hydroquinone in the presence of K_2CO_3 gave dinitrile **4** in 97% yield. The hydrolysis of dinitrile **4** under basic conditions afforded the corresponding dicarboxylic acid **5** in 82% yield. To construct

Received: January 18, 2016
Published: February 24, 2016

DOI: 10.1021/acs.orglett.6b00171
Org. Lett. 2016, 18, 1052–1055

Scheme 1. Synthesis of 3

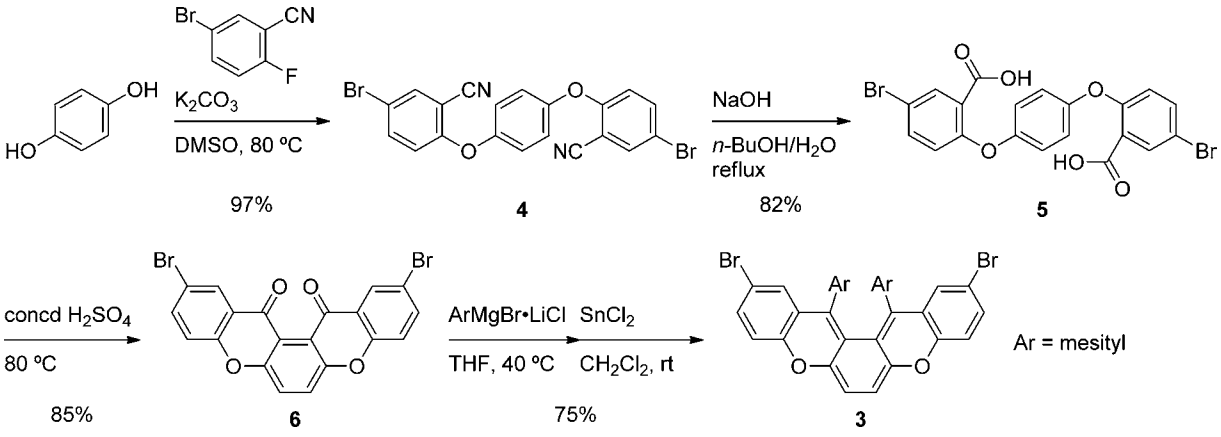

the angular fused-ring framework by acid-catalyzed intramolecular electrophilic cyclization, **5** was heated in concentrated H_2SO_4,[12] regioselectively affording dione **6** as the only product in 85% yield. The origin of this regioselectivity can be explained in terms of the shape of the HOMO in the (9-xanthone)oxidanium cation intermediate, which has a large coefficient at the 8-position (*ortho*-carbon with respect to the carbonyl group, Scheme S1) rather than the 6-position (*para*-carbon).[13] Finally, **6** was converted to the corresponding diol by addition of mesityl Grignard reagent, and then the crude diol was treated with $SnCl_2$ to afford **3** as a dark bluish-purple solid in 75% yield over two steps.

The detailed structure of **3** was obtained from X-ray structural analysis (Figure 2 or S1). Single crystals for X-ray

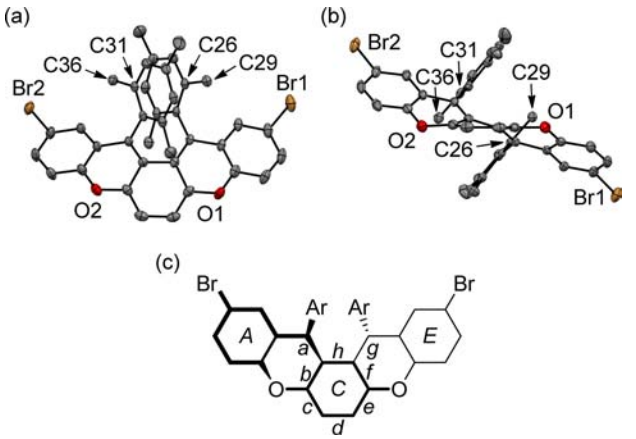

Figure 2. Crystal structure of **3**: (a) top and (b) side views. Hydrogen atoms are omitted for clarity. Thermal ellipsoids set at 50%. (c) Assigned names of the selected bond and ring positions.

analysis were obtained by the slow diffusion of *n*-hexane into the CH_2Cl_2 solution of **3**.[14] The X-ray analysis showed that **3** had a significantly twisted π-framework because of the steric repulsion between the two mesityl groups, in which the distance of the shortest contact was 3.146(3) Å of C26−C31. The twisting angle was estimated to be 64.4° from the dihedral angle between the terminal rings *A* and *E*. The C−C bonds around the central ring *C* showed more distinct bond-length alternation compared to those of **1** and **2**. Namely, bonds *a* (1.359(3) Å), *c* (1.333(3) Å), *e* (1.333(3) Å), and *g* (1.359(3) Å) had double-bond nature, whereas bonds *b* (1.458(3) Å), *d* (1.436(3) Å), *f* (1.461(3) Å), and *h* (1.485(3) Å) had single-bond nature. These bond lengths are consistent with the reported theoretical data of *o*QDM[15] and the experimental data of **2**, clearly indicating that **3** is a homologue of *o*QDM. DFT calculations were carried out for both **3** (twisted form) and **7** (Ar = H, planar form) to elucidate the effect of the twisted structure on the electronic properties of DOP π-system (Figure S2, Tables S2 and S3). DFT calculations (RB3LYP/6-31G**) indicated that **3** and **7** have significantly different LUMO energy levels (**3**: −2.27 eV and **7**: −2.61 eV) and similar HOMO energy levels (**3**: −4.63 eV and **7**: −4.47 eV). These results establish that the twisting structure has a large effect on the LUMO energy levels and minor effect on HOMO energy levels. In addition, the singlet biradical characters were calculated as occupation number of LUMO, 0.091 (9%) for **3** and 0.090 (9%) for **7**, using the CASSCF(2,2)/6-31G//RHF/6-31G** method, showing that the singlet biradical characters were nearly independent of the twisted structure.

At room temperature, the ^{1}H NMR spectrum of **3** in $CDCl_3$ showed three singlet peaks in the aliphatic region attributed to the methyl protons in the mesityl groups (Figure 3b),

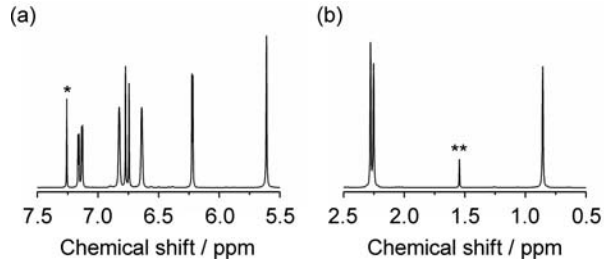

Figure 3. ^{1}H NMR spectrum of **3** in $CDCl_3$ at selected regions: (a) 7.5−5.5 (int ×3) and (b) 2.5−0.5 ppm. *chloroform; **water. See also Figure S3.

indicating the hindered rotation of the mesityl groups due to the steric congestion. Surprisingly, one of the singlet peaks shifted to a higher magnetic field at 0.86 ppm compared to the other methyl singlets (2.28 and 2.25 ppm). Judging from the crystal structure in Figure 2, two sets of *o*-methyl protons on the C29 and C36 are positioned on the facing mesityl rings, thus affecting the ring-current effect. Similar to these mesityl protons, the aromatic protons in the mesityl group were observed as two slightly broadened singlets at 6.83 and 6.64 ppm (Figure 3a). The remaining four peaks (one double−

DOI: 10.1021/acs.orglett.6b00171
Org. Lett. 2016, 18, 1052−1055

doublet, two doublets, and one singlet) in the aromatic region were assigned to the DOP protons, indicating the C_2 symmetry of the DOP unit. The results indicate a twisted structure in the solution state, similar to that observed in the crystal state. The singlet signal at 5.61 ppm can be assigned to the central-ring protons. The corresponding protons of 5,6-dimethylidenecyclohaxa-1,3-diene and 2,2-dimethyl-2*H*-indene appeared at 6.00[16] and 6.08 ppm,[17] respectively. The upfield shift of the observed protons (5.61 ppm) in the central ring *C* in **3** can be partly due to the presence of oxygen atoms at the 5- and 8-positions. Intense cross-peaks were observed for both methyl protons (2.25 and 0.86 ppm) and aromatic protons (6.83 and 6.64 ppm) in the mesityl groups in the NOESY spectrum of **3** in $CDCl_3$ at 298 K, indicating the site exchange due to the flipping of twisted structure (Figure S4). The variable-temperature ^{1}H NMR spectra of **3** in *o*-dichlorobenzene-d_4 showed the coalescence of the methyl protons and the aromatic protons at around 403 and 363 K, respectively (Figure S5). The racemization barrier ($\Delta G^{\ddagger}$) was estimated to be ~75 kJ mol^{-1} by the coalescence method (Table S4).[18]

The UV−vis absorption spectrum of **3** in CH_2Cl_2 showed a broad and intense absorption band in the visible region (450−700 nm, λ_{max} = 560 nm, $\varepsilon = 1.04 \times 10^4$ M^{-1} cm^{-1}) despite the significantly twisted structure (Figure 4). The shape of the

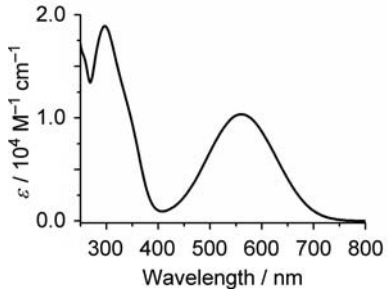

Figure 4. UV−vis absorption spectrum of **3** in CH_2Cl_2.

absorption band of **3** was similar to that reported for Ph_4*o*QDM (λ_{max} = 520 nm, $\lambda_{edge} \approx$ 620 nm).[7] A significant red shift was observed for the visible absorption, indicating that the π-conjugation on the *o*QDM in **3** significantly extended to the terminal benzene rings via two oxygen bridges. The HOMO−LUMO energy gap was estimated as 1.77 eV from the absorption edge. This value is smaller than the HOMO−LUMO energy gap of Ph_4*o*QDM (2.00 eV) and comparable to the reported HOMO−LUMO energy gap of **2** (1.70 eV). Moreover, **3** showed a negligible spectral change for a week under daylight and aerated conditions at room temperature (Figure S6), indicating the high stability of **3**.

The cyclic voltammogram of **3** in CH_2Cl_2 (Figure 5) exhibited two reversible oxidation waves at +0.07 V and +0.42 V vs Fc/Fc$^+$, indicating that the cationic species of **3** were electrochemically stable. In particular, the first oxidation potential indicates its superior electron-donating ability compared to previously reported *o*QDM derivatives (**1**: +0.61 V vs Ag/Ag$^+$, **2**: +0.59 V vs Fc/Fc$^+$). Moreover, one reversible reduction wave was observed at −2.00 V. The electrochemical small HOMO−LUMO energy gap of 1.90 V was estimated from the onset potentials of the oxidation and reduction of **3**.

We carried out the chemical oxidation of **3** for isolating radical cation **3**$^{\bullet+}$. The treatment of a CH_2Cl_2 solution of **3** with a 1 equiv amount of tris(4-bromophenyl)aminium hexafluoro-

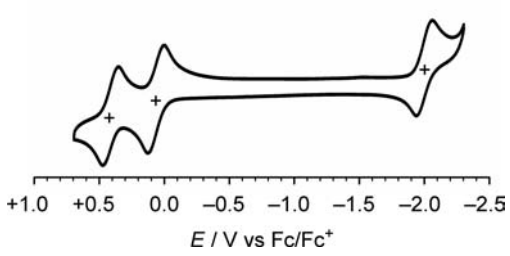

Figure 5. Cyclic voltammogram of **3** in CH_2Cl_2 containing 0.1 M *n*-Bu_4NPF_6 as a supporting electrolyte at a scan rate of 100 mV s^{-1}.

antimonate afforded the desired radical cation salt **3**$^{\bullet+}$·SbF_6^- as a dark blue solid. This solid is stable under aerated conditions at room temperature. The UV−vis−NIR spectrum of **3**$^{\bullet+}$·SbF_6^- was measured in CH_2Cl_2 (Figure 6). The observed spectrum is

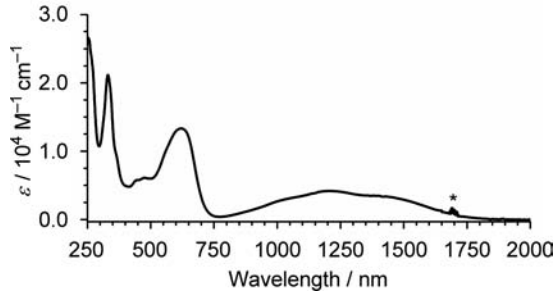

Figure 6. UV−vis−NIR spectrum of **3**$^{\bullet+}$·SbF_6^- in CH_2Cl_2. *Solvent peaks.

consistent with that observed by the electrochemical oxidation (Figure S7). Radical cation salt **3**$^{\bullet+}$·SbF_6^- showed the characteristic broad NIR absorption up to 1800 nm that can be assumed as a charge-resonance band associated with the SOMO−LUMO transition by the means of TD-DFT calculations (Figure S8 and Table S5).

The electron-spin resonance (ESR) spectrum of **3**$^{\bullet+}$·SbF_6^- in degassed CH_2Cl_2 at room temperature showed a 1:2:1 triplet line resulting from the hyperfine coupling with two equivalent ^{1}H nuclei (I = 1/2) with g = 2.0038 (Figure 7). The observed

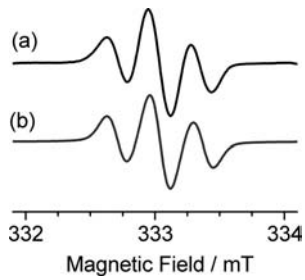

Figure 7. (a) Observed and (b) simulated ESR spectra of **3**$^{\bullet+}$·SbF_6^- in CH_2Cl_2 at room temperature. Parameters for simulation: g = 2.0038, $|a^{1H}|$ (×2) = 0.330 mT.

ESR spectrum was reproduced by spectral simulation with an estimated hyperfine coupling constant of $|a^{1H}|$ = 0.330 mT. The results confirm that the electron spin density was mainly localized in the *o*QDM moiety. The calculated spin density is consistent with the experimental results (Figure S9).

In conclusion, we have designed and synthesized a stable *o*QDM derivative **3** with a highly twisted structure in both the

DOI: 10.1021/acs.orglett.6b00171
Org. Lett. 2016, 18, 1052−1055

crystal and solution state. Compound **3** showed bond-length alternation and a broad visible absorption, characteristic of an *o*QDM structure. Moreover, **3** was shown to be a superior electron donor. Furthermore, we successfully isolated the radical cation salt $\mathbf{3}^{\bullet+}\cdot SbF_6^-$ and disclosed the detailed electronic structure by spectroscopic measurements. The fundamental properties of the DOP π-system **3** are summarized as follows: a colored substance with a high stability and a superior electron donor, affording a stable radical cation based on the *o*QDM structure. By introducing additional functional groups at the terminal Br-attached carbons, further elongation of absorptions is possible. Furthermore, replacing the mesityl groups with further bulky groups would enable the optical resolution of *o*QDM structures. The synthesis of various π-conjugated systems based on the DOP framework is in progress in our laboratory.

■ ASSOCIATED CONTENT

Supporting Information

The Supporting Information is available free of charge on the ACS Publications website at DOI: 10.1021/acs.orglett.6b00171.

Synthesis and characterization of all new compounds, spectral data, details of computational studies, and crystallographic data for **3** (PDF)

■ AUTHOR INFORMATION

Corresponding Authors

*E-mail: kozaki@sci.osaka-cu.ac.jp.
*E-mail: okadak@sci.osaka-cu.ac.jp.

Notes

The authors declare no competing financial interest.

■ ACKNOWLEDGMENTS

This work was partially supported by Grant-in-Aid for Scientific Research from JSPS (No. 26288041 to K.O.) and financial support Grant-in-Aid for Scientific Research on Innovative Areas "π-System Figuration: Control of Electron and Structural Dynamism for Innovative Functions" from MEXT (No. 26102005 to S.S.). C.S. also thanks the financial support by the Sasakawa Scientific Research Grant from The Japan Science Society.

■ REFERENCES

(1) Electronics: (a) Brütting, W.; Adachi, C. *Physics of Organic Semiconductors*, 2nd ed.; Wiley−VCH: Weinheim, 2012. Magnetism and spintronics: (b) Itoh, K.; Kinoshita, M. *Molecular Magnetism*; Kodansha & Gordon and Breach: Tokyo, 2000. Molecular devices:. (c) Feringa, B. L.; Browne, W. R. *Molecular Switches*, 2nd ed.; Wiley−VCH: Weinheim, 2011.

(2) For example, see: (a) Patai, S.; Rappoport, Z. *The Chemistry of the Quinonoid Compounds*; Wiley: Chichester, 1988; Vol. 2. (b) Inoue, S.; Aso, Y.; Otsubo, T. *Chem. Commun.* **1997**, 1105−1106. (c) Kurata, H.; Inase, M.; Oda, M. *Chem. Lett.* **1999**, *28*, 519−520. (d) Sun, Z.; Ye, Q.; Chi, C.; Wu, J. *Chem. Soc. Rev.* **2012**, *41*, 7857−7889. (e) Kubo, T. *Chem. Lett.* **2015**, *44*, 111−122.

(3) Tetracyano-*p*-QDM (TCNQ) and its analogues were studied as organic conductors: (a) Martin, N.; Segura, J. L.; Seoane, C. *J. Mater. Chem.* **1997**, *7*, 1661−1676. (b) Hünig, S.; Herberth, E. *Chem. Rev.* **2004**, *104*, 5535−5563. (c) Saito, G.; Yoshida, Y. *Bull. Chem. Soc. Jpn.* **2007**, *80*, 1−137. Recently, *p*QDM-fused systems have received attention as organic field effect transistors. See: (d) Chase, D. T.; Fix, A. G.; Kang, S. J.; Rose, B. D.; Weber, C. D.; Zhong, Y.; Zakharov, L. N.; Lonergan, M. C.; Nuckolls, C.; Haley, M. M. *J. Am. Chem. Soc.* **2012**, *134*, 10349−10352. (e) Nishida, J.; Tsukaguchi, S.; Yamashita, Y. *Chem. - Eur. J.* **2012**, *18*, 8964−8970. (f) Mori, T.; Yanai, N.; Osaka, I.; Takimiya, K. *Org. Lett.* **2014**, *16*, 1334−1337.

(4) See, for example: (a) Yamaguchi, S.; Hanafusa, T.; Tanaka, T.; Sawada, M.; Kondo, K.; Irie, M.; Tatemitsu, H.; Sakata, Y.; Misumi, S. *Tetrahedron Lett.* **1986**, *27*, 2411−2414. (b) Kurata, H.; Tanaka, T.; Oda, M. *Chem. Lett.* **1999**, *28*, 749−750. (c) Kikuchi, A.; Iwahori, F.; Abe, J. *J. Am. Chem. Soc.* **2004**, *126*, 6526−6527. (d) Tonzola, C. J.; Hancock, J. M.; Babel, A.; Jenekhe, S. A. *Chem. Commun.* **2005**, 5214−5216. (e) Zhu, X.; Tsuji, H.; Nakabayashi, K.; Ohkoshi, S.; Nakamura, E. *J. Am. Chem. Soc.* **2011**, *133*, 16342−16345.

(5) (a) Charlton, J. L.; Alauddin, M. M. *Tetrahedron* **1987**, *43*, 2873−2889. (b) Segura, J. L.; Martin, N. *Chem. Rev.* **1999**, *99*, 3199−3246. (c) Yoshida, H.; Ohshita, J.; Kunai, A. *Bull. Chem. Soc. Jpn.* **2010**, *83*, 199−219.

(6) Yoshida, S.; Fujii, M.; Aso, Y.; Otsubo, T.; Ogura, F. *J. Org. Chem.* **1994**, *59*, 3077−3081.

(7) Quinkert, G.; Wiersdorff, W. W.; Finke, M.; Opitz, K.; von der Haar, F. G. *Chem. Ber.* **1968**, *101*, 2302−2325.

(8) (a) Iwashita, S.; Ohta, E.; Higuchi, H.; Kawai, H.; Fujiwara, K.; Ono, K.; Takenaka, M.; Suzuki, T. *Chem. Commun.* **2004**, 2076−2077. (b) Suzuki, T.; Sakano, Y.; Iwai, T.; Iwashita, S.; Miura, Y.; Katoono, R.; Kawai, H.; Fujiwara, K.; Tsuji, Y.; Fukushima, T. *Chem. - Eur. J.* **2013**, *19*, 117−123.

(9) In terms of Clar's sextet rule, the dibenzo annulation results in the dominant contribution of the biphenyl-type resonance structure where two exocyclic double bonds are separated from the aromatic sextet: Portella, G.; Poater, J.; Solà, M. *J. Phys. Org. Chem.* **2005**, *18*, 785−791.

(10) Shimizu, A.; Tobe, Y. *Angew. Chem., Int. Ed.* **2011**, *50*, 6906−6910.

(11) (a) Clifton, M. F.; Fenick, D. J.; Gasper, S. M.; Falvey, D. E.; Boyd, M. K. *J. Org. Chem.* **1994**, *59*, 8023−8029. (b) Okada, K.; Imakura, T.; Oda, M.; Kajiwara, A.; Kamachi, M.; Yamaguchi, M. *J. Am. Chem. Soc.* **1997**, *119*, 5740−5741.

(12) (a) Badger, G. M.; Pettit, P. *J. Chem. Soc.* **1952**, 1874−1877. (b) Ullmann, F.; Maag, R. *Ber. Dtsch. Chem. Ges.* **1906**, *39*, 1693−1696.

(13) (a) Watanabe, M.; Suzuki, H.; Tanaka, Y.; Ishida, T.; Oshikawa, T.; Tori-i, A. *J. Org. Chem.* **2004**, *69*, 7794−7801. (b) Yamada, S.; Iwama, S.; Kinoshita, K.; Yamazaki, T.; Kubota, T.; Yajima, T. *Tetrahedron* **2014**, *70*, 6749−6756.

(14) Crystallographic data for **3**: triclinic, space group: *Pn* (#2), a = 9.037(4) Å, b = 12.111(5) Å, c = 13.963(6) Å, α = 84.843(15)°, β = 77.598 (10)°, γ = 88.338(11)°, V = 1486.4 (11) Å^3, Z = 2, ρ_{calcd} = 1.516 g cm^{-3}, T = 150 K, R_1 = 0.0291, R_w = 0.0437, GOF = 0.945. CCDC 1440146 contains the supplementary crystallographic data for this paper. These data can be obtained free of charge from the Cambridge Crystallographic Data Center via www.ccdc.cam.ac.uk/data_request/cif.

(15) (a) Gleicher, G. J.; Newkirk, D. D.; Arnold, J. C. *J. Am. Chem. Soc.* **1973**, *95*, 2526−2531. (b) Said, M.; Maynau, D.; Malrieu, J. P.; Bach, M. A. G. *J. Am. Chem. Soc.* **1984**, *106*, 571−579. (c) Sakai, S. *J. Phys. Chem. A* **2000**, *104*, 11615−11621.

(16) Trahanovsky, W. S.; Chou, C. H.; Fischer, D. R.; Gerstein, B. C. *J. Am. Chem. Soc.* **1988**, *110*, 6579−6581.

(17) (a) Dolbier, W. R., Jr.; Matsui, K.; Michl, J.; Horak, D. V. *J. Am. Chem. Soc.* **1977**, *99*, 3876−3877. (b) Johansson, E.; Skramstad, J. *J. Org. Chem.* **1981**, *46*, 3752−3754.

(18) (a) Williams, D. H.; Fleming, I. *Spectroscopic Methods in Organic Chemistry*, 5th ed.; McGraw-Hill: London, 1995. (b) Hesse, M.; Meier, H.; B., Zeeh *Spectroscopic Methods in Organic Chemistry*, 2nd ed.; Thieme: Stuttgart, 2007.

DOI: 10.1021/acs.orglett.6b00171
Org. Lett. 2016, 18, 1052−1055